JOURNAL OF MATERIALS SCIENCE 20(1985) 2767–2775

The initiation of crack growth in linear polyethylene

S. K. BHATTACHARYA, N. BROWN
Department of Materials Science and Engineering, Laboratory for Research on the Structure of Matter, University of Pennsylvania, Philadelphia, PA 19104, USA

The initiation of crack growth was observed in single edge notched tensile specimens under plane strain conditions. The shape of the deformation zone varied from being balloon-like above 12 MPa and nearly planar below but neither shape conformed to that predicted by the conventional shear type yield criteria. The initial damaged zone grew at a constant velocity with a stress dependence of $V = V_0\sigma^n$. The spectrum of damage morphologies that preceed crack growth consists of a leading edge of crack-like pores followed by a region of increasing fibrillation which is terminated by a region of increasing fibril fracture.

1. Introduction

Little is known about crack initation in polyethylene (PE). There are many studies of crack growth and extensive studies of time to failure in an engineering structure such as a gas pipe. Chan and Williams [1], Ewing *et al.* [2], Popelar and Staab [3], Lee and Epstein [4], Uralil and Markham [5] have measured crack growth as a function of the stress intensity, K. A detailed study by Chan and Williams [1] showed that there was a range of crack growth rates V, which was controlled by K where

$$V = AK^n$$

The various studies produced n values of 4 to 9. Chan and Williams [1] found that the initiation stage of crack growth was not simply described by the above equation. Bragaw [6] found that observable crack growth was preceded by an incubation time which represented a significant part of the total time to failure in a gas pipe.

This paper is a continuation of a research programme to understand the phenomenology and microstructural changes that occur during the initiation of crack growth in PE. In previous work by Bhattacharya and Brown [7, 8] the microstructural aspects of crack initiation were explored. It was found that the first evidence of damage at the root of notch consisted of an array of crack-like pores. With increasing time the damaged zone grew until the following regions developed: the crack-like porosity came first which gradually transformed to a fibrillated region and finally, the region of fibril fracture. Previously Bandyopadhyay and Brown [9] had identified a fractured and craze-like region in PE but did not make a distinction between the fibrillated and crack-like pores. In this paper further details of the transition from the porous to the fibrillated region will be presented.

In addition to the observations of the microstructure, the dependence of the size of the damaged zone on stress, time and depth of the initiating notch was determined. The test specimen was single edge notch tension type whose geometry produced plane strain conditions. The effects of plane stress were determined by comparing the damaged zones at the surface and within the interior of the specimen. It was found that the damage zone developed more rapidly in the interior where plane strain prevailed. The length and width of the damaged zone increased linearly with time under a constant stress. For stresses above about 1/2 the yield point, the width of the damage zone increased markedly so that it transformed from a planar zone to one that was balloon shaped at the highest stresses.

0022–2461/85 $03.00 + .12

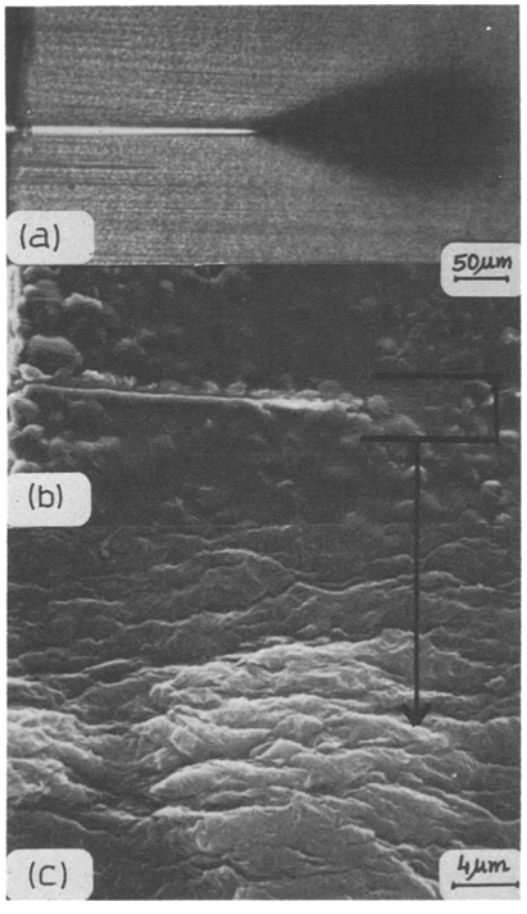

Figure 1 (a) Transmitted light micrograph. (b) SEM of surface etched with permanganic acid. (c) Same as (b).

2. Experimental details

The polyethylene was the same unpigmented commercial resin used in previous investigations [7, 8]. It was Marlex 6006 which was supplied and compression moulded by the Phillips Petroleum Company in accordance with ASTM D1928 and cooled at 15° C min^{-1}. The moulded plaques were 4.5 mm thick, melt index 0.75; $M_n = 19\,600$, $M_w = 130\,000$ and a density of 0.964 gm cm^{-3}. The PE has a yield point of 25 MPa at 300 K and at a strain rate of 0.02 min^{-1}.

The details of notching the specimen were presented in a previous paper [8]. Most notches were about 0.250 mm deep and 15 mm long corresponding to the width of the tensile specimen. The notching technique was especially controlled so that the deformed region at the root of the notch was negligible relative to the subsequent damaged zone produced by loading the specimen. As described previously only two notches were cut per razor blade and the notching speed was 0.02 mm min^{-1}.

The depth of the damaged zone plus the depth of the original notch was generally less than 1/10th the thickness of the specimen. The width of the specimen, 15 mm, was such that over 95% of the notch was exposed to plane strain deformation. The values of stress intensity, K, for the single edge notched tensile specimen were obtained from Paris and Sih [10] where

$$K = 1.12(\pi^{1/2})\sigma a^{1/2}$$

where σ is the applied stress and a is the notch depth.

Three types of microscopic observations were made. Thin slices about 0.2 mm thick were obtained with a razor blade from the interior of the specimen and observed under transmitted light as in Fig. 1a. Special care was taken to slice without modifying the damaged zone. Slices about 5 mm thick were fractured in liquid nitrogen to expose the plane of the notch and the damaged zone and then observed with the SEM (Fig. 2). Surfaces from the interior of the specimen and perpendicular to the length of the notch were etched with permanganic acid according to procedures by Bassett and Hodge [11] and modified by Naylor and Phillips [12] and observed with the SEM (Figs. 1b and c).

3. Results

3.1. Effect of exterior surface

When crack growth is observed by viewing the external surface of the specimen, there is an apparent incubation time because the crack appears first on the inside before it becomes visible. Fig. 3 shows the damaged zone after it has been exposed by fracturing in liquid nitrogen. It is seen that the extent of the damaged zone is less at the exterior than the interior of the specimen, and at about 0.3 mm from the exterior surface the extent of the damaged zone is constant. Fig. 4 shows thin slices taken at various distances from the external surface which support the observations from Fig. 3. In general these observations show that damaged zones consisted of porous, fibrillated, and fractured regions, but the extent of these regions is less at the exterior surface when compared with the damaged zone that forms internally under plane strain.

Since the edge effect, which represents the transition from plane stress to plane strain, takes

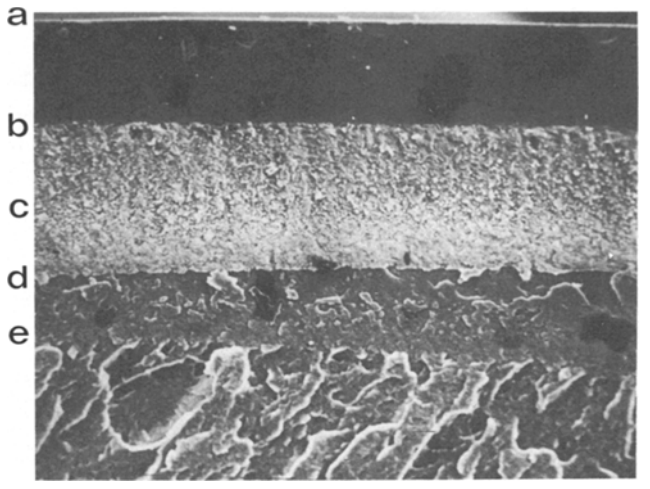

Figure 2 SEM of damaged zone after fracture in liquid nitrogen: a–b is notched; b–c fractured region; c–d fibrillated; d–e porous; beyond e virgin material.

place over a distance of about 0.3 mm, then about 96% of the 15 mm wide specimen was exposed to plane strain conditions.

3.2. Effect of stress, time and notch depth

Fig. 5 gives an overview of how the damaged zone depends on stress and time. Below about 12 MPa the damaged zone remains narrow irrespective of time. Above 12 MPa both the width and length of the damaged zone increase with stress and time. The narrow part of the damaged zone next to the notch corresponds to a fractured region where the stress has relaxed. Fig. 6 shows more details of a damaged zone in a specimen exposed to 22 MPa for 5 min.

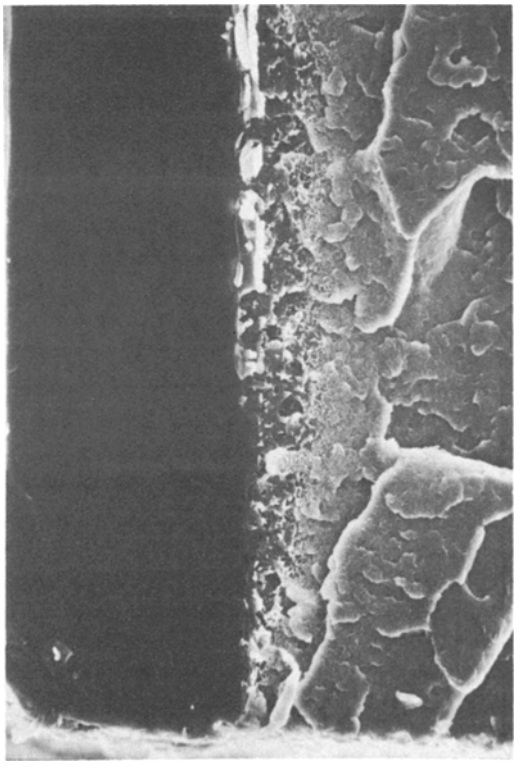

Figure 3 Damaged zone after fracture in liquid nitrogen. Right edge of micrograph is exterior surface of specimen where plane stress occurs.

Figs. 7 and 8 show the length and maximum width of the damaged zone as a function of the applied stress for various times of application and for a 0.25 mm deep notch. For stress less than 12 MPa the width remains constant and then rapidly increases to produce the balloon shape.

Figs. 9 and 10 show the increase in length and width of the damaged zone with time for a constant stress. There is a linear relationship for all stresses. For zero time, which corresponds to rapidly loading and unloading the specimen within 1 sec, an instantaneous zone of damage is produced.

The growth of the damaged zone at a constant velocity as shown in Figs. 9 and 10, was obtained for short times of testing. Fig. 11 shows that for a stress of 10 MPa, the constant velocity persisted for 600 min even though the damage zone had become equal to the length of the original notch.

Fig. 12 shows how the length of the damage zone varies with the length of the original notch for stresses from 6.2 to 20.5 MPa and for loading times of about 1.0 min. The data shows considerable scatter, but as expected the damaged zone increases with stress and notch depth. In the discussion, these results will be compared with the Dugdale prediction.

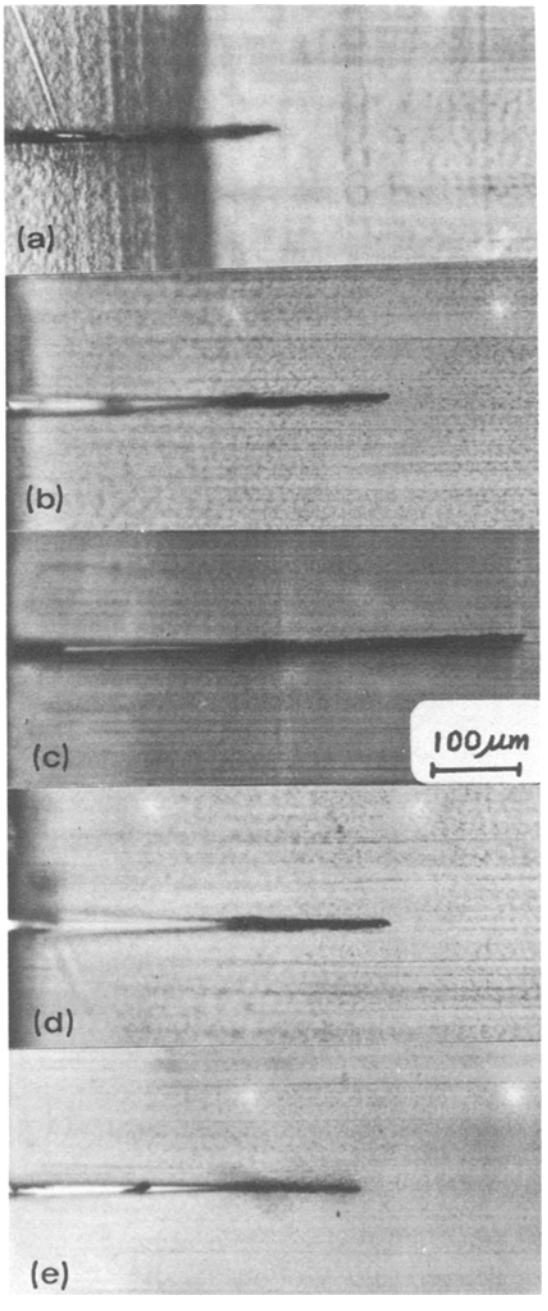

Figure 4 Transmitted light micrographs of thin slices taken at various distance from external surface of the specimen. Shows edge effect.

3.3. Microstructure of the damaged zone

Figs. 1b and c show the nature of the deformation in the leading region of the damaged zone. The damage consists of wavy crack-like pores. They are called crack-like because they are thin and mostly perpendicular to the applied tensile stress. This porous region is the first evidence of damage at the root of a notch.

Fig. 13 shows how the damaged zone looks after rapid fracture in liquid nitrogen. The root of the razor-blade notch is at a. From a to b is the region of crack growth. From b to c is a fibrillated region and c to d is the transition region from fibrillation to the crack-like pores shown in Figs. 1b and c. From d to e is the undamaged region.

4. Discussion

4.1. Shape of the damaged zone

If the rate of crack growth is based on a surface observation, then an incubation time is expected since the crack grows faster in the interior as shown in Figs. 3 and 4. This is only a superficial effect which stems from the fact that a crack grows differently under plane stress than under plane strain. However, it is of interest to consider the difference in the effects of plane stress and plane strain on the damaged zone.

According to the conventional view point (Knott [13]), for a solid that obeys the Tresca or von Mises yield criterion, the plastic zone is larger for plane stress than plane strain. Also the plastic zone has a wing shape under plane strain but is kidney shaped for plane stress. The damaged zones in Fig. 5 were all produced under plane strain conditions but there is no evidence of the conventional wing shape predicted by the Tresca or von Mises criterion. A calculation was made of the shape that would be predicted when the von Mises criterion is modified by the hydrostatic component of the stress. The modified von Mises criterion as presented by Bowden and Jukes [14] is given by

$$\frac{1}{6^{1/2}}[(\sigma_1-\sigma_2)^2+(\sigma_2-\sigma_3)^2 + (\sigma_3-\sigma_1)^2]^{1/2} = \tau_y-\mu P$$

where τ_y is the yield point in pure shear, and $P=(\sigma_1+\sigma_2+\sigma_3)/3$ is the hydrostatic component of the stress and μ is a constant whose value is about 0.04 for PE according to Bowden and Jukes [14]. Even for values of μ about 0.2 the calculated shape was not in accord with Fig. 5 where the deformation zones tend to follow the plane of the notch rather than to form wings about the notch. A survey of the literature indicated that the yield criterion for PE under plane strain conditions is not well established. The fact that the deformation zone under plane strain tends to be in the plane of the notch especially at low stresses indicates that

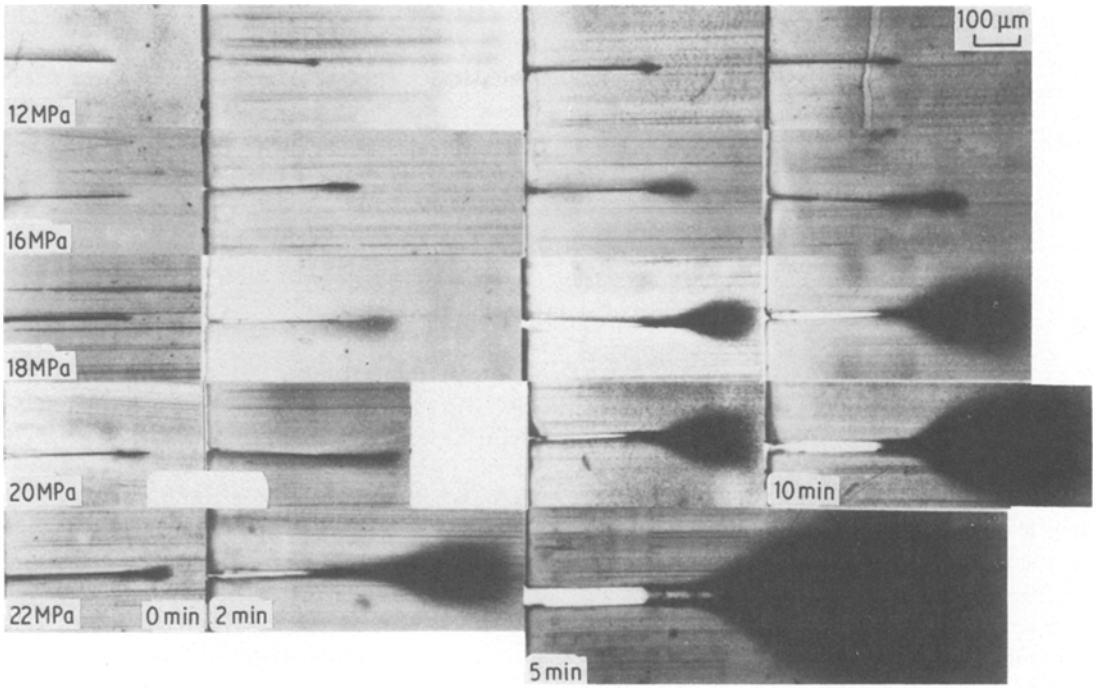

Figure 5 Shows how damaged zone depends on stress and time at 25° C. Notch depth = 0.25 mm.

the yield criterion may be more closely connected with the maximum tensile stress than with a shear type of criterion.

The growth of the crack is expected to occur more widely under plane strain as discussed by Knott [13] because the hydrostatic component is greater than under plane stress. This is in accord with our observations even though the shape of the deformation region of the damaged zone does not conform to the conventional criteria for yielding.

Fig. 5 shows that at a stress above about 12 MPa the width of the damaged zone begins to increase relatively to its length. The width depends on time. The spreading of the damage zone in two dimensions represents the onset of large scale yielding. Macroscopically a similar effect occurs when a pipe is exposed to an internal pressure.

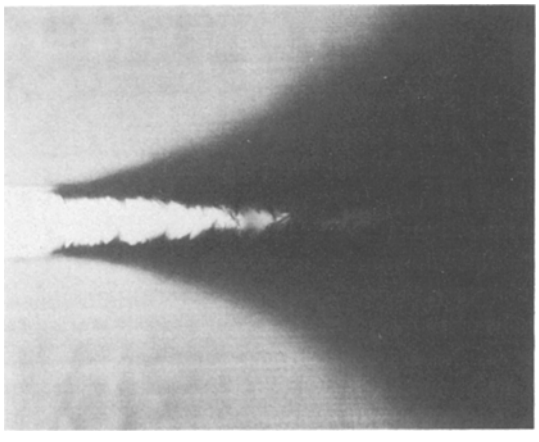

Figure 6 Details of damaged zone exposed to 22 MPa for 5 min at 25° C.

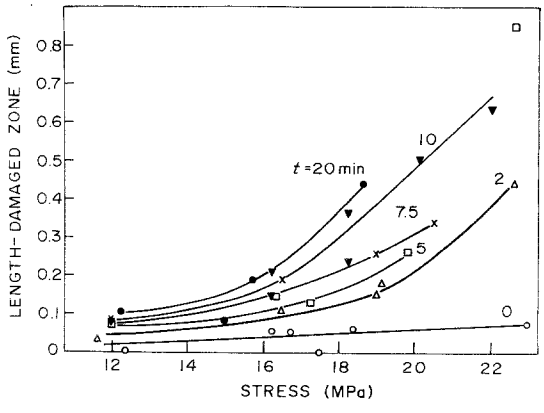

Figure 7 Length of damaged zone against stress for various times. Notch depth = 0.25 mm.

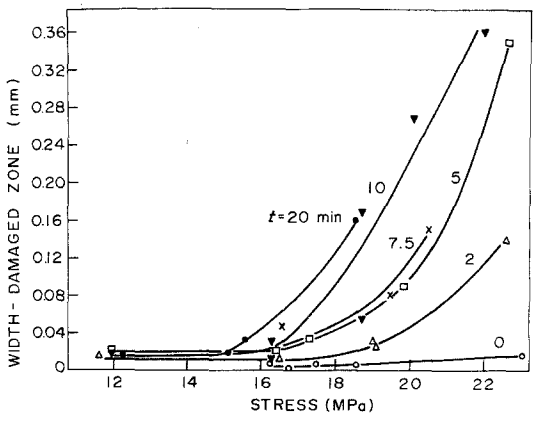

Figure 8 Same as Fig. 7 but width against stress.

Above a critical stress, depending on the temperature, the pipe bulges before it leaks, whereas below this stress, the pipe exhibits a brittle failure from a slit type crack. Why PE exhibits the balloon shaped deformation zone under plane strain is not understood but it appears that the time dependence of the deformation should be taken into account.

4.2. Velocity of the damaged zone

Both the length and width of the damaged zone increase linearly with time as shown in Figs. 9 to 11. It is surprising that the damaged zone has a constant velocity during its initiation stage because the spectrum of morphologies along its length is changing. A constant velocity is not expected while the character and length of the deformation zone are changing. Vitek [15] has given a general theory of the initiation of creep crack growth. In the theory, the strain along the deformation zone changes as its length increases and consequently the stress distibution along the deformation zone changes with time. Vitek assumed that the relationship between strain rate and stress was the same along the deformation zone but since the stress varied, the deformation zone was not predicted to grow at a constant velocity. In the case of PE it is not expected that the relationship between strain rate and stress is the same for the porous region and the fibrillated region and it is expected that the local stress would vary along the deformation zone; consequently a constant velocity for the deformation zone is not anticipated. An explanation can only be supplied by a detailed micromechanics analysis of the initiation process based on a knowledge of the constitutive relationships for the morphological states that constitute the damaged zone.

As shown in Figs. 9 to 11, the damaged zone can grow at a constant velocity almost to the size of the orginal notch. It is surprising that the size of the original notch seems to control the velocity of the damaged zone when its leading edge is so far removed from the tip of the notch. Once the fractured region develops then the velocity of the crack is described by $V = AK^n$ where K is the instantaneous stress intensity as shown by Chan and Williams [1] and Popelar and Staab [3].

All the data in Figs. 9 and 10 are for a notch depth of 0.25 mm. When the velocities of the damaged zone from Figs. 9 and 10 are plotted against the stress, then the following relationships are obtained for lengthening and widening respectively

$$v_l = 6.4 \times 10^{-9}\, \sigma^{5.0}\, \text{mm min}^{-1}$$

$$v_w = 0.1 \times 10^{-9}\, \sigma^{6.3}\, \text{mm min}^{-1}$$

Thus, it is seen that the widening velocity is more

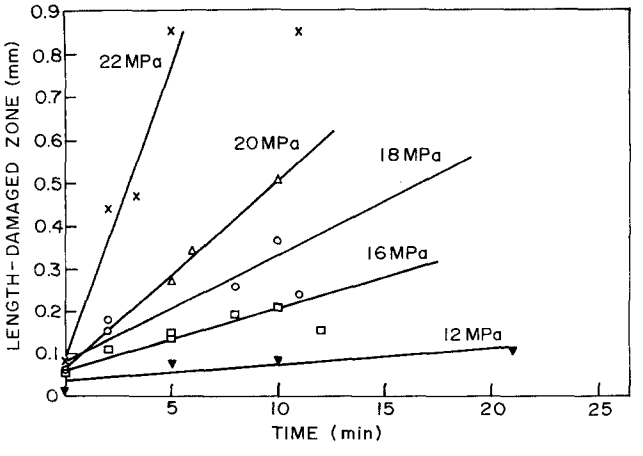

Figure 9 Length of damaged zones against time at constant stress. Notch depth = 0.25 mm.

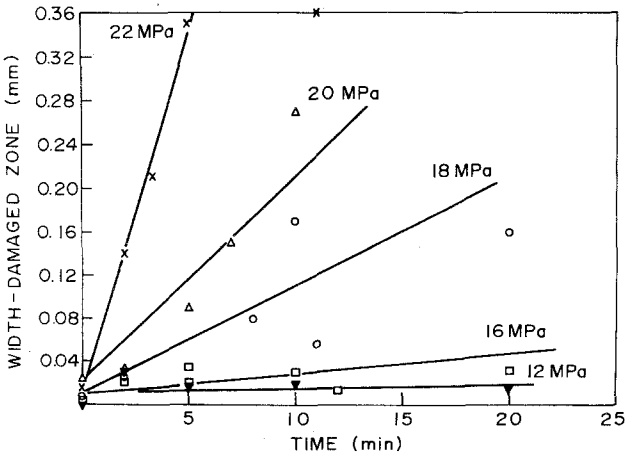

Figure 10 Same as Fig. 9 but width against time.

sensitive to an increase in stress than is the lengthening. In the limit as the stress approaches the yield point both widening and lengthening velocity should become equal since the deformation occurs over the entire specimen. Setting $v_l = v_w$ in the above equations gives a stress of 25 MPa which is the yield point of the material as expected.

4.3. Comparison of short time damaged zone with the Dugdale prediction

The length of the damaged zone as a function of notch depth in Fig. 12 shows roughly a linear relationship. Since the measurements were made for a short time of loading, it is of interest to compare these observations with the prediction of the Dugdale model [16]. For an elastic–plastic non-work hardening solid, the Dugdale model predicts that the size of the plastic zone at the root of a sharp crack is given by:

$$\Delta = \frac{\pi}{8}\frac{K^2}{\sigma_y^2}$$

where K is the stress intensity, and σ_y is the yield point. In our particular case $\sigma_y = 25$ MPa. Thus $\Delta/k^2 = 0.50 \times 10^{-3}$ MPa^{-2}. The data in Fig. 12 give $\Delta/k^2 = 1.0 \times 10^{-3}$ MPa^{-2}. Thus, the experimental values are approximately equal to the Dugdale model, but is somewhat larger possibly because PE is very time dependent and does not behave as a simple non-work hardening elastic–plastic solid.

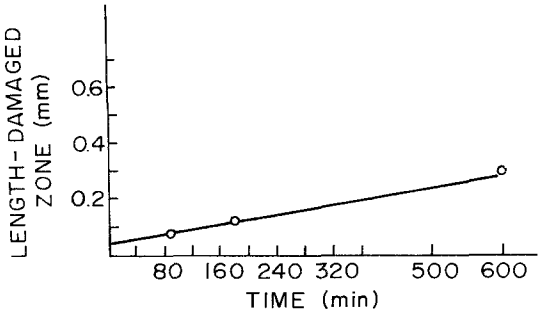

Figure 11 Length of damage zone against time at 25° C and 10 MPa.

4.4. Microstructure of the damaged zone

All the microstructural evidence suggests that the typical damaged zone may be depicted as in Fig.

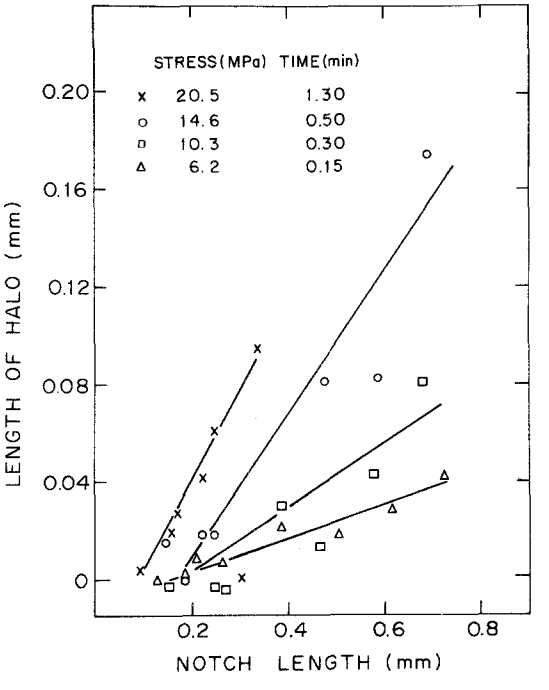

Figure 12 Length of damaged zone halo against depth of orginal notch for various stresses and short times of about 1 min.

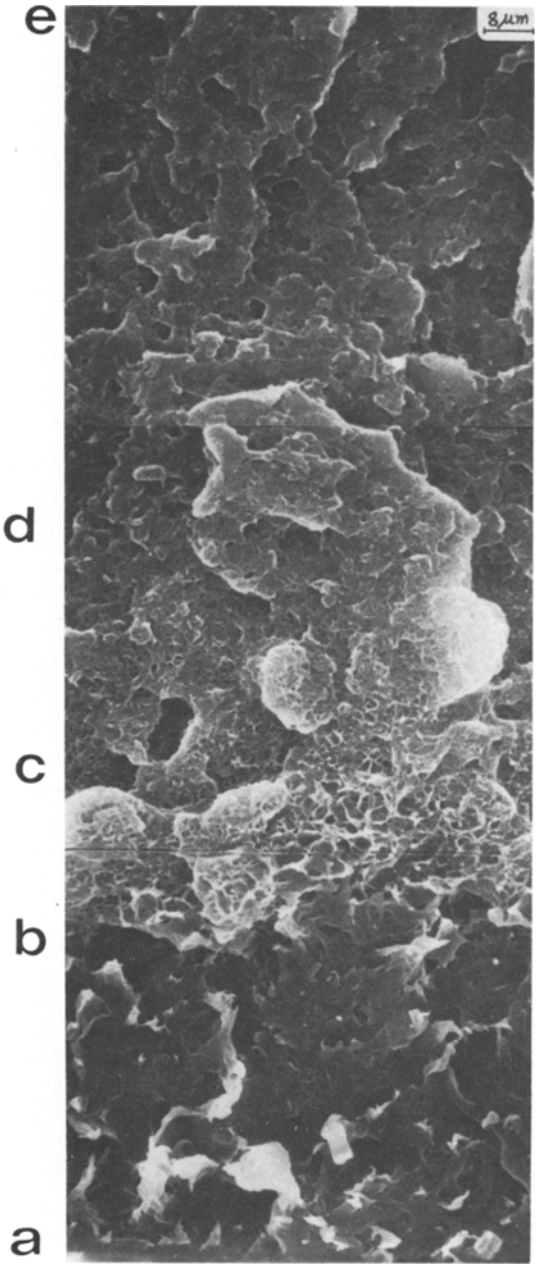

Figure 13 Like Fig. 2 but a higher magnification. a–b fractured zone, b–c fibrillated, c–d transition from fibrillation to crack-like pores, d–e virgin material.

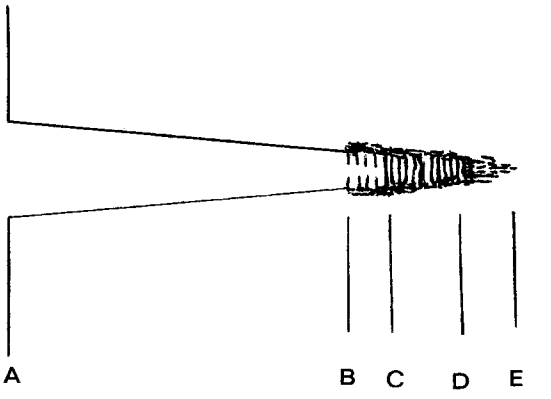

Figure 14 Schematic of damaged zone. A–B notch; B–C fractured; C–D fibrillated; D–E porous.

14. A–B is the original notch, B–C is the fractured region; C–D is the fibrillated region and D–E the porous region. The extent of each region depends on stress, time and length of the original notch. During steady state crack growth it is expected that region C–E would increase as the size of the crack increases.

When the damaged zone is fractured in liquid nitrogen, the SEM micrograph of Fig. 2 is obtained where the regions A to E correspond to those depicted in Fig. 14. The fracture path is planar as long as the fibrillated zone offers a homogeneous fracture resistance to the rapid crack in liquid nitrogen. When the liquid nitrogen crack arrives at the region of discontinuous porosity, then it ceases to be planar and advances along pathways of least resistance. Thus the region C–E in Fig. 2 is expected to have a mottled appearance.

5. Summary

1. Below 12 MPa the damage zone is essentially planar.

2. Above 12 MPa the width of the damaged zone increases rapidly relative to its length.

3. The dimensions of the damaged zone increase linearly with time.

4. The velocity of the damaged zone depends on stress according to $V = A\sigma^n$ where A and n depend on direction of the zone.

5. Fig. 14 depicts the range of morphologies that constitute the damaged zone during crack initiation under plane strain conditions.

Acknowledgements

The research was sponsored by the Gas Research Institute. Research facilities were provided by the Laboratory for Research on the Structure of Matter which is supported by the National Science Foundation.

Discussions with Professor J. L. Bassani and Professor V. Vitek were extremely helpful. The calculations on the shape of the deformation zone were made by Mr L. Fager.

References

1. M. K. V. CHAN and J. G. WILLIAMS, *Polymer* **24** (1983) 234.
2. L. EWING, J. M. GRIEG and D. WALTON, Proceedings of the Sixth Plastic Symposium, Columbus, Ohio, April 1978 (American Gas Association, Arlington, USA, 1978) p. 2.
3. C. H. POPELAR and G. H. STAAB, Eighth Plastic Pipe Symposium, New Orleans, November 1983 (American Gas Association, Arlington, USA, 1983) p. 62.
4. C. S. LEE and M. M. EPSTEIN, *Polym. Eng. Sci.* **22** (1982) 549.
5. F. S. URALIL and R. L. MARKHAM, Eighth Plastic Fuel Gas Pipe Symposium New Orleans, November 1983 (American Gas Association, Arlington, USA, 1983) p. 10.
6. C. G. BRAGAW, Proceedings of the Sixth Plastic Symposium Columbus, Ohio, April 1978 (American Gas Association. Arlington, USA, 1978) p. 36.
7. S. K. BHATTACHARYA and N. BROWN, Eighth Plastic Pipe Symposium (American Gas Association, Arlington, USA, 1983) p. 58.
8. *Idem*, *J. Mater. Sci.* **20** (1984) 2519.
9. S. BANDYOPADHYAY and H. R. BROWN, Proceedings of 3rd International Conference on mechanical Behavior of Materials, Vol. 3 (American Society of Metals, 1979).
10. P. C. PARIS and C. G. SIH, ASTM TP No. 381 (American Society for Testing and Materials, Philadelphia, 1965) p. 30.
11. D. C. BASSETT and A. M. HODGE, *Proc. Roy. Soc.* **A377** (1981) 25.
12. K. L. NAYLOR and P. J. PHILLIPS, *J. Polym. Sci.* **21** (1983) 2011.
13. J. F. KNOTT, "Fundamentals of Fracture Mechanics" (Butterworths, London, Boston, 1973) Chap. 5.
14. P. B. BOWDEN and J. A. JUKES, *J. Mater. Sci.* **7** (1972) 52.
15. V. VITEK, *Int. J. Fract.* **13** (1977) 39.
16. D. S. DUGDALE, *J. Mech. Phys. Solids* 8 (1960) 100.

Received 9 July
and accepted 31 July 1984